esa

ECOSPHERE

Three novel methods to estimate abundance of unmarked animals using remote cameras

Anna K. Moeller,[1,]† Paul M. Lukacs,[1] and Jon S. Horne[2]

[1]*Wildlife Biology Program, Department of Ecosystem and Conservation Sciences, W.A. Franke College of Forestry and Conservation, University of Montana, Missoula, Montana 59812 USA*
[2]*Idaho Department of Fish and Game, Lewiston, Idaho 83501 USA*

Citation: Moeller, A. K., P. M. Lukacs, and J. S. Horne. 2018. Three novel methods to estimate abundance of unmarked animals using remote cameras. Ecosphere 9(8):e02331. 10.1002/ecs2.2331

Abstract. Abundance and density estimates are central to the field of ecology and are an important component of wildlife management. While many methods exist to estimate abundance from individually identifiable animals, it is much more difficult to estimate abundance of unmarked animals. One step toward noninvasive abundance estimation is the use of passive detectors such as remote cameras or acoustic recording devices. However, existing methods for estimating abundance from cameras for unmarked animals are limited by variable detection probability and have not taken full advantage of the information in camera trapping rate. We developed a time to event (TTE) model to estimate abundance from trapping rate. This estimate requires independent estimates of animal movement, so we collapsed the sampling occasions to create a space to event (STE) model that is not sensitive to movement rate. We further simplified the STE model into an instantaneous sampling (IS) estimator that applies fixed-area counts to cameras. The STE and IS models utilize time-lapse photographs to eliminate the variability in detection probability that comes with motion-sensor photographs. We evaluated the three methods with simulations and performed a case study to estimate elk (*Cervus canadensis*) abundance from remote camera trap data in Idaho. Simulations demonstrated that the TTE model is sensitive to movement rate, but the STE and IS methods are unbiased regardless of movement. In our case study, elk abundance estimates were comparable to those from a recent aerial survey in the area, demonstrating that these new methods allow biologists to estimate abundance from unmarked populations without tracking individuals over time.

Key words: abundance; *Cervus canadensis;* density; elk; exponential distribution; Poisson point process; remote camera; space to event; time-lapse photography; time to event; unmarked population.

Received 16 May 2017; accepted 18 May 2018. Corresponding Editor: Debra P. C. Peters.

† **E-mail:** anna.moeller@umontana.edu

Introduction

Knowledge of species' abundance is integral to managing and conserving populations (Williams et al. 2002). Passive detectors, such as remote cameras, are gaining popularity for estimating abundance noninvasively (O'Connell et al. 2011). However, most camera studies have applied capture–recapture models that require individually identifiable animals (Karanth 1995, Burton et al. 2015). Many species have no natural markings to allow individual identification, so animals must be physically captured and marked, which can be invasive, expensive, and logistically challenging (Chandler and Royle 2013). Promising models to estimate abundance of unmarked individuals include *N*-mixture models (Royle 2004), the Spatial Count (SC) model (Chandler and Royle 2013), the Random Encounter Model (REM) (Rowcliffe et al. 2008), and a distance sampling (DS) model (Howe et al. 2017). However, the parameters of *N*-mixture models can be

non-identifiable without auxiliary data (Barker et al. 2017) and estimates can be biased high if animals are detected at multiple cameras (Keever et al. 2017) or if detection probability is <0.5 (Dénes et al. 2015). The SC model produces imprecise estimates even under ideal circumstances unless it is supplemented with auxiliary data (Chandler and Royle 2013, Sollmann et al. 2013). The REM is recognized as a promising model, but its broad applicability is still being tested (Rovero and Marshall 2009, Manzo et al. 2012, Zero et al. 2013, Cusack et al. 2015, Balestrieri et al. 2016, Caravaggi et al. 2016). Likewise, the DS model remains to be tested in various field situations (Howe et al. 2017).

One of the challenges for estimating abundance using cameras that several of these methods try to address is variable detection by motion sensors. Motion-sensor sensitivity can change with the animal's size, distance, and angle of approach, as well as environmental variables such as ambient temperature and obstructive vegetation (Rowcliffe et al. 2011, Burton et al. 2015). If variable detection is ignored, the area in front of the camera can be hard to calculate, which can bias abundance estimates from models that depend on it, like the REM. A fact that seems to be largely ignored is that most remote cameras are capable of taking photographs at regular intervals. Methods that take advantage of time-lapse photographs can be advantageous because they do not need explicitly to model motion-sensor variability. We developed two such methods that use time-lapse photographs in order to decrease uncertainty in detection. While time-lapse photographs may not be suitable for rare species that are difficult to capture on camera, they can be ideal for more common species that are of conservation or management concern.

Another source of information from cameras that has been largely overlooked is the timing of detections (Bischof et al. 2014). Time to event (TTE) models are a natural fit for cameras because they record events continuously. Time-to-event, or survival, models are used in fields as diverse as industry, medicine, and ecology (Muenchow 1986). In ecology, they can be used to estimate survival of animals (Cox and Oakes 1984), quantify predator–prey encounters (Whittington et al. 2011), and determine survey effort (Garrard et al. 2008). It has long been noted that trapping rate increases as abundance increases (Carbone 2001, Rowcliffe et al. 2008, Rovero and Marshall 2009). While using trapping rate as an index of abundance is controversial (Carbone 2001, 2002, Jennelle et al. 2002), it can be highly useful if used as an estimator of abundance (Rowcliffe et al. 2008).

To utilize time of detection data, we developed a TTE model to estimate abundance from trapping rate. Because trapping rate varies not only with abundance, but also with animal movement rates and variable detectability rate (Jennelle et al. 2002, Parsons et al. 2017), we propose ways to take these into account. The resulting model approaches the REM and has similar assumptions and limitations. Like the REM, it requires independent estimates of movement rate, which can be difficult to attain without telemetry data (Bradshaw et al. 2007). To address the issue of movement, we propose a novel take on the TTE framework. By collapsing the sampling intervals to an instant in time, we create a space to event (STE) model whose abundance estimates are unaffected by animal movement rate. This model is based in the same theory but substitutes space for time. The STE model utilizes time-lapse photographs, which eliminates the impact of variable detection on estimates of density. We further simplify this model into an instantaneous sampling (IS) estimator that has more flexible assumptions of animal distribution but requires accurate counts of animals.

We demonstrated use of these three models through simulation and estimation of wintering elk (*Cervus canadensis*) abundance through cameras. We believe these methods are highly applicable to species such as elk that are relatively common and are difficult or expensive to survey. In the United States, many management agencies seek to maximize elk harvest while maintaining a healthy population; abundance estimates can be crucial when setting harvest quotas. However, elk are most commonly counted through aerial surveys, and aviation accidents are the largest threat to wildlife biologists' safety (Sasse 2003). Because the methods described here rely on random camera placement and/or time-lapse photographs, they can be quite suitable for common species that produce lots of pictures. In some cases, these design requirements can help cut

down the number of photographs that need to be analyzed, increasing efficiency when estimating abundance.

Methods

Time to event model

At a randomly placed motion-triggered camera, the time until the target species is detected is a function of abundance, movement rate, and detectability (Jennelle et al. 2002, Parsons et al. 2017). The TTE model uses this fact to estimate abundance from observations of the time (starting from any arbitrary moment) until an animal is first detected. In this framework, we separate the two components of the detection process: availability and perception. Frequently, in camera trap literature, these two processes are combined so that detection is defined as the probability of detecting an animal given it is in a plot that is sampled by a camera (Burton et al. 2015). We do away with the idea of sampling an entire plot with a camera and instead focus only on the area within the camera's viewshed. In this way, we reduce the definition of detection probability to the probability that an animal is captured by a motion-triggered camera, given the animal is in the camera's viewshed. We begin by formulating the TTE model assuming perfect detection, and then, we present an extension to account for variable detectability.

We begin with a photograph stream from a single camera, which we divide into multiple sampling occasions (e.g., one day = one sampling occasion). We then divide each sampling occasion into consecutive sampling periods (e.g., 24 one-hour periods; Fig. 1). We model the number of animals N_{ijk} in view at camera $i = 1, 2, \ldots, M$ on occasion $j = 1, 2, \ldots, J$ and period $k = 1, 2, \ldots, K$, as

$$N_{ijk} \sim \text{Pois}(\lambda) \quad (1)$$

where λ is the average number of animals in view at a camera.

In a TTE framework, we are interested in estimating λ by observing T, the number of sampling periods until the first animal encounters the camera. For a single observation of TTE T_{ij} at camera $i = 1, 2, \ldots, M$ and sampling occasion $j = 1, 2, \ldots, J$, we record the first sampling period $k = 1, 2, \ldots, K$ in which we observe the species of interest (Fig. 2). For example, at camera 1 on day 1, if we first observe the species of interest in the third sampling period, we record the TTE $T_{11} = 3$. If we do not observe an animal by the end of the Kth sampling period, the TTE must be longer than our observation time, so we right-censor this occasion (Muenchow 1986, Pyke and Thompson 1986, Castro-Santos and Haro 2003, Bischof et al. 2014). An example encounter history at camera 1 with $J = 5$ and $K = 24$ for each sampling occasion may look like $T_{1j} = \{NA, 23, NA, NA, 5\}$, where a right-censored sampling occasion is represented by NA.

In order to account for movement rate, we set the length of the sampling period equal to the average length of time it takes for an animal to cross through the camera's field of view. In field settings, this requires an independent estimate of movement rate. In our simulations and case study, we use an approximation of the time it takes animals to move through the camera and

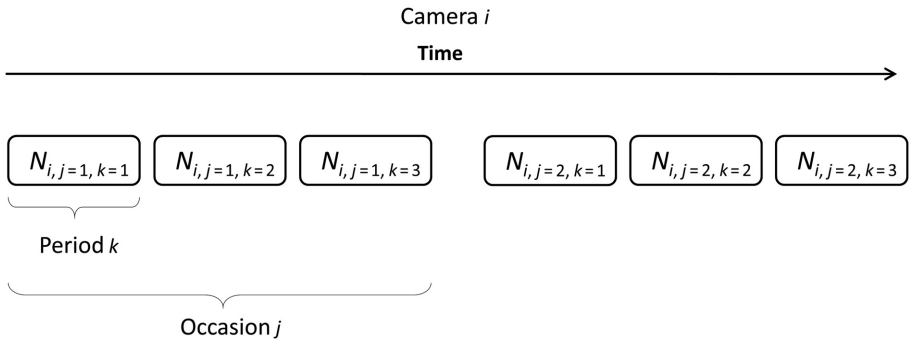

Fig. 1. Schematic of sampling periods and occasions for the time to event model. At camera $i = 1, 2, \ldots, M$, sampling occasion $j = 1, 2, \ldots, J$ is broken into several sampling periods $k = 1, 2, \ldots, K$. Here, $J = 2$ and $K = 3$.

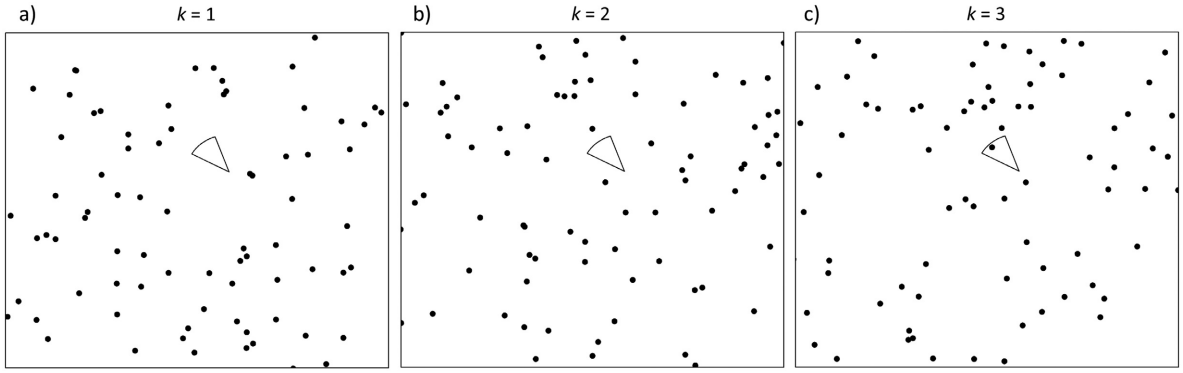

Fig. 2. Conceptual diagram of the time to event (TTE) model. The circular sector is the viewshed of a single camera i on a single occasion j divided into three successive sampling periods (a–c). The black dots represent randomly placed animals. The observed TTE T_{ij} is equal to the period k in which the camera first contains an animal. There are no animals in the camera in (a) $k = 1$ or (b) $k = 2$, but there is an animal in the camera in (c) $k = 3$, so for this camera and sampling occasion, $T_{ij} = 3$.

we encourage future work to tease apart the exact relationship between movement rate and camera size. After accounting for movement in this way, and assuming perfect detection, the observed TTE (measured by the number of sampling periods until an animal is detected) is based only on abundance. Since TTE is based only on abundance, we can estimate λ using the relationship between the Poisson and exponential distributions. When an event of interest is Poisson-distributed, the interval between events is an exponential random variable (Berkson 1975, Hutchinson and Waser 2007, de Smith 2015). Therefore, the observed T follows the exponential distribution

$$T \sim \text{Exp}(\lambda) \tag{2}$$

where λ is equal to the parameter in Eq. 1. We estimate λ (the average number of animals in a camera) from the exponential likelihood, including right-censored data (indicated by $(1 - I_{(T_{ij} \le K)})$) by integrating over the upper tail of the probability density function. The full likelihood for λ given the encounter history T_{ij} over $i = 1, 2, \ldots, M$ cameras on $j = 1, 2, \ldots, J$ sampling occasions with $k = 1, 2, \ldots, K$ sampling periods per occasion is

$$\mathcal{L}(\lambda|T_{ij}) = \prod_{j=1}^{J}\prod_{i=1}^{M}\begin{pmatrix} I_{(T_{ij} \le K)}\lambda e^{-\lambda T_{ij}} \\ +(1 - I_{(T_{ij} \le K)})e^{-\lambda T_{ij}} \end{pmatrix} \tag{3}$$

giving us $\hat{\lambda}$, the average number of animals in the camera's viewshed. We can estimate overall density ($\hat{D}$) by dividing by the mean area of a camera's viewshed $\bar{a}$:

$$\hat{D} = \frac{\hat{\lambda}}{\bar{a}} \tag{4}$$

Mean camera area $\bar{a}$ is calculated as $\bar{a} = 1/M \sum_{i=1}^{M} a_i$. The viewable area a_i for each camera is the circular sector defined by the lens angle (θ_i) in degrees and the trigger distance (r_i), following

$$a_i = \pi r_i^2 \frac{\theta_i}{360} \tag{5}$$

We can convert density to total abundance N by multiplying by the area of the sampling frame A

$$\hat{N} = \hat{D}A \tag{6}$$

We estimate the sampling variance of $\hat{N}$ using the properties of maximum likelihood theory and the delta method (Mood et al. 1974, Oehlert 1992, Williams et al. 2002). R code for implementing the TTE model is given in Data S1 and Appendix S1.

Because the TTE method uses replicates in both space and time, we can model heterogeneous density by adding a linear model to λ_i, the average density at camera i, in the general form

$$\log(\lambda_i) = \beta_0 + \beta_1 x_{1i} + \beta_2 x_{2i} \tag{7}$$

where x_i are a site-specific covariates. When modeling heterogeneous density, we must constrain the number of sampling periods per sampling occasion so that each observed TTE arises from the abundance in the area immediately around

each camera. The longer we sample, the larger the effective sampling area becomes; animals farther and farther away from the camera are added to the population at risk of capture. Therefore, we must keep the number of sampling periods small (e.g., $K = 3$) to meet this assumption.

To account for imperfect detection at the camera level for the TTE model, we suggest an extension using the geometric and gamma distributions. A camera with imperfect detection may miss an animal on its first z visits to a camera, but the camera will capture it on the $(z + 1)$th visit. The sum of exponential waiting times is gamma-distributed, so the waiting time until the $(z + 1)$th visit is a gamma-distributed random variable (Mood et al. 1974). The full likelihood of λ uses observations of T_{ij}, the gamma-distributed TTE at camera $i = 1, 2, \ldots, M$ on occasion $j = 1, 2, \ldots, J$ with $k = 1, 2, \ldots, K$ sampling periods per occasion. It also uses z, a geometric-distributed count of the number of sampling periods missed. Right-censored occasions are indicated by $1 - I_{(T_{ij} \le K)}$ when there are no observations by the end of the Kth sampling period in sampling occasion j. The full likelihood in the shape-rate formulation is

$$\mathcal{L}(\lambda|T_{ij}) = \prod_{j=1}^{J}\prod_{i=1}^{M}\sum_{z=0}^{\infty}\begin{pmatrix} I_{(T_{ij}\le K)}p(1-p)^z\frac{\lambda_i^{z+1}}{\Gamma(z+1)}T_{ij}^z e^{-\lambda_i T_{ij}} \\ +(1-I_{(T_{ij}\le K)})p(1-p)^z\left(1-\frac{1}{\Gamma(z+1)}\gamma(z+1,\ \lambda_i T_{ij})\right)\end{pmatrix} \quad (8)$$

where $\Gamma(z + 1)$ is the gamma function $\Gamma(z + 1) = z!$ and $\gamma(z + 1, \lambda_i T_{ij})$ is the lower incomplete gamma function $\gamma(z+1,\ \lambda_i T_{ij}) = \int_0^{\lambda_i T_{ij}} t^z e^{-t} dt$. Further development of the geometric-gamma formulation is needed because there is a near singularity in the Hessian matrix. In this paper, we demonstrate the TTE model formulated under perfect detection only.

Space to event model

Because the TTE model requires estimates of movement rate in order to set the sampling periods appropriately, we developed the STE model that does not require this auxiliary information. The STE model is conceptually similar to the TTE model, but we collapse each sampling occasion to an instantaneous sample. Because of this, the estimates are independent of animal movement rate. As with the TTE model, we begin by modeling the number of animals in view of a camera using the Poisson distribution (1). However, instead of observing the time until we observe an animal using the exponential distribution, we can instead collect data on the amount of space S between animals. As with the TTE model, when events of interest are Poisson-distributed, the interval (of space in this case) between them is exponentially distributed $S \sim \text{Exp}(\lambda)$ (de Smith 2015).

In order to estimate the amount of space between animals, we take observations of random areas of the landscape at an instant in time. If an observer were to repeatedly draw random areas of the landscape until they found an animal, the so-called STE would be the total area sampled until that point. Because the sample is instantaneous, the mean STE $E[S] = 1/\lambda$ depends only on the number of animals, so we can estimate density without any further constraints. When using time-lapse photographs, detection probability is defined as the probability that an animal is captured and correctly identified given it is in the camera's viewshed. As with the TTE model, we develop this model assuming perfect detection, which we address further in the discussion.

To observe S in practice, we randomly deploy time-lapse cameras that take photographs at predefined times. As opposed to the TTE model, where we split sampling occasions into sampling periods, we now define sampling occasions as a single instant in time. At each sampling occasion $j = 1, 2, \ldots, J$ (e.g., every 1 h), we observe a snapshot of the number of animals in view of each camera. We record the STE as the total area sampled before an animal is first observed.

As an example, we examine all the photographs taken at a single time ($j = 1$). We first calculate the area of each camera following Eq. 5. Since we are using time-lapse cameras instead of motion-sensor cameras, the maximum distance r is defined by field landmarks rather than the trigger distance. After randomly ordering the cameras, we look through the photographs until we find the first animal detection. If camera 1 (with area a_1) contains at least one animal, we record the space to first event

$S_{j=1} = a_1$. If, instead, camera 1 is empty but camera n contains at least one animal, we record $S_{j=1} = a_1 + a_2 + \ldots + a_n$ (Fig. 3). An example encounter history with $J = 5$ with average camera area $\bar{a} = 30\,\text{m}^2$ may look like $S_j = \{180\ \text{m}^2, 30\ \text{m}^2, NA, 300\ \text{m}^2, NA\}$, where a right-censored sampling occasion is represented as NA.

Once we have observed our encounter history S_j for $j = 1, 2, \ldots, J$ sampling occasions over $i = 1, 2, \ldots, M$ cameras, we estimate λ with the exponential likelihood, following the TTE model with one fewer dimension

$$\mathcal{L}(\lambda|S_j) = \prod_{j=1}^{J}\left(I_{(S_j \le M)}\lambda e^{-\lambda S_j} + \left(1 - I_{(S_j \le M)}\right)e^{-\lambda S_j}\right) \tag{9}$$

where $I_{S_j \le M}$ indicates that an animal was seen in at least one camera. Because the STE model looks at events in space, censored occasions occur when no animals were observed in the M cameras. Because we have already factored in the camera area, λ now represents density. To extrapolate to abundance, we multiply by the sampling frame area, as in Eq. 6. We calculate the variance of $\hat{N}$ using the estimated information matrix and the delta method (Mood et al. 1974, Oehlert 1992, Williams et al. 2002).

Instantaneous sampling estimator

If we count the animals in view at each photograph taken for the STE model, we essentially have a fixed-area count repeated in space and time. The IS estimator uses counts of animals from randomly deployed time-lapse cameras. Over many spatial and temporal replicates, the mean count n_{ij} at location $i = 1, 2, \ldots, M$ and occasion $j = 1, 2, \ldots, J$ is an estimate of density ($\hat{D}$) when divided by the cameras' viewable area (a_{ij}), following

$$\hat{D} = \frac{1}{J} \cdot \frac{1}{M} \sum_{j=1}^{J} \sum_{i=1}^{M} \frac{n_{ij}}{a_{ij}} \tag{10}$$

We can convert to abundance following Eq. 6.

Because fixed-area point counts are special cases of fixed-area transects, we estimated variance of the parameter $\hat{D}$ based on the formula for random line transects of unequal lengths (Thompson 2002, Fewster et al. 2009), following:

$$\widehat{\text{Var}}(\hat{D}) = \frac{M}{L^2(M-1)} \sum_{i=1}^{M} (J \cdot a_i)^2 \left(\frac{n_i}{J \cdot a_i} - \frac{n}{L}\right)^2 \tag{11}$$

where Ja_i is the summed area of camera i across all occasions, $L = \sum_{i=1}^{M} J \cdot a_i$, count n_i is the count of animals over all occasions at camera i, and n is

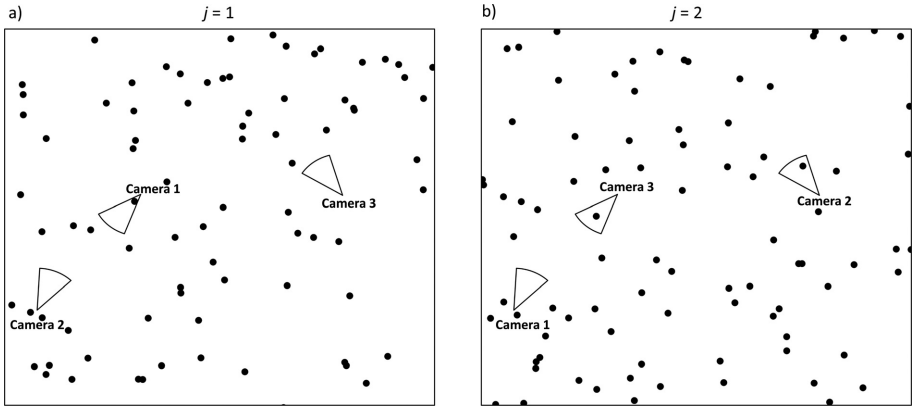

Fig. 3. Conceptual diagram of the space to event (STE) model. The circular sectors represent three different cameras on two different occasions (a–b). On each occasion $j = 1, 2, \ldots, J$, we randomly order the cameras $i = 1, 2, \ldots, M$. If the first animal detection is in the nth camera, the observed STE S_j is the sum of the areas of cameras 1, 2, … n. (a) On occasion $j = 1$, camera 1 contains at least one animal, so we record the space to first event $S_{j=1} = a_1$. (b) On occasion $j = 2$, cameras 2 and 3 both contain animals, but we use the first camera in the series. Therefore, we record the space to first event $S_{j=1} = a_1 + a_2$.

the total count of animals over all cameras and occasions. We then estimated the variance of $\hat{N}$ using the delta method.

Assumptions

All three abundance estimators assume demographic and geographic closure of the study area, random camera placement, and independent observations of animals. To meet the closure assumptions, an appropriate sampling frame and time should be chosen during which the population is closed to birth, death, immigration, and emigration. While the models assume demographic and geographic closure on the level of the sampling frame, it is important to note that they do not assume geographic closure at the plot level, as *N*-mixture models do (Royle 2004). Second, cameras should be deployed randomly across the landscape rather than targeting features such as roads or trails (Rowcliffe et al. 2013). Animals should be neither attracted to nor repelled by the cameras, so sites should be unbaited and minimally disturbed. Next, detections of animals are assumed to be independent in space and time. As long as cameras are randomly deployed, the properties of random sampling mean that animals captured at one camera are not any more or less likely to step in front of the next camera. However, it is slightly more difficult to address independence of animal detections at a single camera. We should consider animal behavior when defining sampling occasions and leave enough time for animals to redistribute across the landscape. We can help address independence of detections by selecting sampling occasions randomly or systematically, but we still may see autocorrelation across observations. In these cases, bootstrapping may help to appropriately estimate the variance.

The TTE and STE models assume that animals follow a Poisson distribution at the spatial scale of the camera. If animals are clumped due to landscape features, we could incorporate covariates on λ to help address extra variance on the landscape. Additionally, the TTE model requires an independent estimate of the average amount of time for an animal to move through the camera area. These estimates can be obtained through auxiliary data like global positioning system (GPS) collars.

All models are currently formulated under the assumption that detection probability is 1. When using time-lapse photographs, as in the STE and IS methods, this may be fairly reasonable. The cameras take photographs at specified intervals regardless of whether they detect an animal. As long as the view in front of the camera is appropriately clear and photograph viewers are consistently trained, the photographs reflect a true capture history of animal presence and absence. On the other hand, motion-sensor cameras pose a larger issue for detection. Because detection probability decreases with distance (Rowcliffe et al. 2011, Howe et al. 2017), the user may want to use only those photographs with animals a short distance from the camera so they can assume perfect detection probability. We encourage future work into extending these models when $P < 1$.

Simulations

We performed mechanistic simulations to evaluate the estimates of abundance and the variances of those estimates for all three models. We simulated slow and fast movement rates for populations of 10 animals and 100 animals. Every individual took an independent uncorrelated random walk for 1000 steps with fixed step lengths (length 1 for the slow population and length 3 for the fast population) and random turning angles, bounded within a 30×30 unit area. Animals were captured at a given time in any of the 10 randomly placed 1×1 unit square cameras if their coordinates fell within the camera's coordinates, inclusive of two borders.

For the IS and STE methods, we created encounter histories based on the number of animals in each camera at every tenth time step. For the IS method, we used the count of animals in the cameras at each sampled time. For the STE method, we created a randomly ordered list of the cameras at each sampled time step and recorded the number of the first camera that contained at least one animal during that time. For the TTE model, we sampled animals during 10-step sampling occasions (each step represented a sampling period in the sampling occasion). We left 10 steps between the end of one sampling occasion and the beginning of the next. At each camera and sampling occasion, we recorded the number of steps until the first animal was caught in the camera.

We ran 1000 simulations for each combination of step lengths (fast and slow) and population

size (10 and 100). We calculated standard error on each estimate using the analytical standard error formulas and delta method. To verify our estimates of standard error, we also calculated the standard deviation of the abundance estimates from the repeated simulations.

Case study: estimating elk abundance

To demonstrate use of these methods in the field, we used a dataset from 80 remote cameras deployed during February 2016. We deployed these cameras in the Beaverhead Mountains of Idaho on a mix of public and private land, with permission from the landowners. The study area was defined by a 2 km buffer around 3525 GPS locations from 18 December 2014 to 20 March 2015 from 33 calf and female elk. This area was characterized by high desert grass–sagebrush communities and windswept hills, where elk movement was mostly unrestrained by topography or dense vegetation. We compared estimates from our models against abundance estimates from a February 2009 aerial survey that was conducted in this area and corrected for sightability bias (Samuel et al. 1987, 1992). We recognize that this is not true abundance, but it serves as a ballpark figure against which to compare our estimates.

Within the sampling frame, we randomly selected nine plots using generalized random-tessellation stratified (GRTS) sampling (Stevens and Olsen 2004) with the R package spsurvey (Kincaid and Olsen 2017, R Core Team 2015). Generalized random-tessellation stratified sampling allows the user to replace plots in the ordered sample, so we replaced two plots due to lack of accessibility during winter and/or lack of landowner approval (Stevens and Olsen 2004). We divided each 1.5 × 1.5 km plot into nine equal sections and systematically placed one camera in each section. Within the bounds of the 500 × 500 m sub-plot, we attempted to place the camera to maximize capture of elk. However, in this study area, a 500 × 500 m sub-plot is relatively homogeneous, and field observations suggested that elk movement was fairly unrestrained at this scale. Thus, while subjective placement at the sub-plot level does not adhere to perfect random sampling, we do not believe we violated the assumption severely. When placing cameras, we made sure that no two cameras were on the same road, trail, or ridge, in order to reduce autocorrelation across cameras. Due to lack of trees, we placed the cameras on T-posts at an approximate height of 4–5 feet. We pointed cameras north to limit direct sunlight in the frame and cleared any vegetation obstructing the camera's view. The infrared flash, motion-triggered cameras (models HC600, PC800, and PC900; Reconyx, Holmen, Wisconsin, USA) had high trigger sensitivity and took bursts of five pictures with no delay between trigger activations. In addition to the motion trigger, cameras took pictures every five minutes from 06:00 to 18:00.

We calculated the visible camera area by camera specifications (TrailcamPro 2017) using Eq. 5. We based visible camera area on the Reconyx HC600 model, letting $\theta = 42°$. The cameras had long, unimpeded views, so we set $r = 50$ m to reduce misclassification and miscounting. We only counted elk within that distance, which we identified by flagging placed in the field.

For the TTE model, we estimated the sampling period length as 1 h. We estimated the distance across a camera as 30 m and calculated elk speed from 1746 locations from 53 GPS collars in the Beaverhead area from January 2015 (IDFG, *unpublished data*). Median elk speed was approximately 30 m/h (including times of foraging and rest), so we set the sampling period length to one hour. At each camera, we sampled for four hours (four 1-h sampling periods), beginning every eight hours throughout February 2016. On each sampling occasion, we recorded the first period in which an elk was detected. If no elk were detected during a given sampling occasion, we right-censored that occasion.

For the STE model, we created a randomly ordered list of cameras and recorded the first camera that detected elk at each sampling occasion. Although the sampling should be instantaneous, we defined the sampling period as 1 min to ensure we had enough detections. Any photographs of elk during that one minute counted as a detection. We sampled each camera for one minute every hour, from 1 February to 13 February 2016. We selected this time frame to ensure that elk were not migrating on or off winter range. If no cameras observed elk at a given sampling occasion, we right-censored that occasion.

For the IS estimator, we counted all visible elk in a subset of photographs taken between 1 February and 29 February 2016. We used

photographs taken on the hour, every hour, so as to reduce autocorrelation between samples. If no photograph was taken on a given occasion, we recorded the count as zero. Ideally, when using repeated fixed-area counts, the spatial replicates should be re-randomized each time. However, with the IS estimator, cameras are not redeployed at each sampling occasion j, so the variance estimator should account for potential correlation among counts at the same camera. Because most analytic variance estimators can be biased low when samples are correlated, we wanted to test the performance of our estimator against the estimate of standard error from a non-parametric bootstrap (Efron and Tibshirani 1993). We created 1000 new datasets by sampling the cameras with replacement and taking all counts at those cameras. We estimated abundance with each dataset. We estimated the standard error of $\hat{N}$ with the standard deviation of these repeated estimates.

Results

Simulations

We tested the three methods on two populations moving at different speeds in populations of two sizes to determine whether movement rate or density influenced abundance estimates (Fig. 4). Simulation results are summarized in Table 1. The TTE model appeared to underestimate abundance for all simulated populations. In both high and low densities, coverage of the TTE's 95% confidence intervals was higher for the faster population than the slow population. This demonstrated that the TTE model is sensitive to movement rate. On the other hand, coverage was approximately equal for the STE and IS models in all simulations. This signaled that the IS and STE models appear to be unbiased regardless of movement rate or population density.

The delta method appeared to underestimate variance for the TTE model, which contributed to

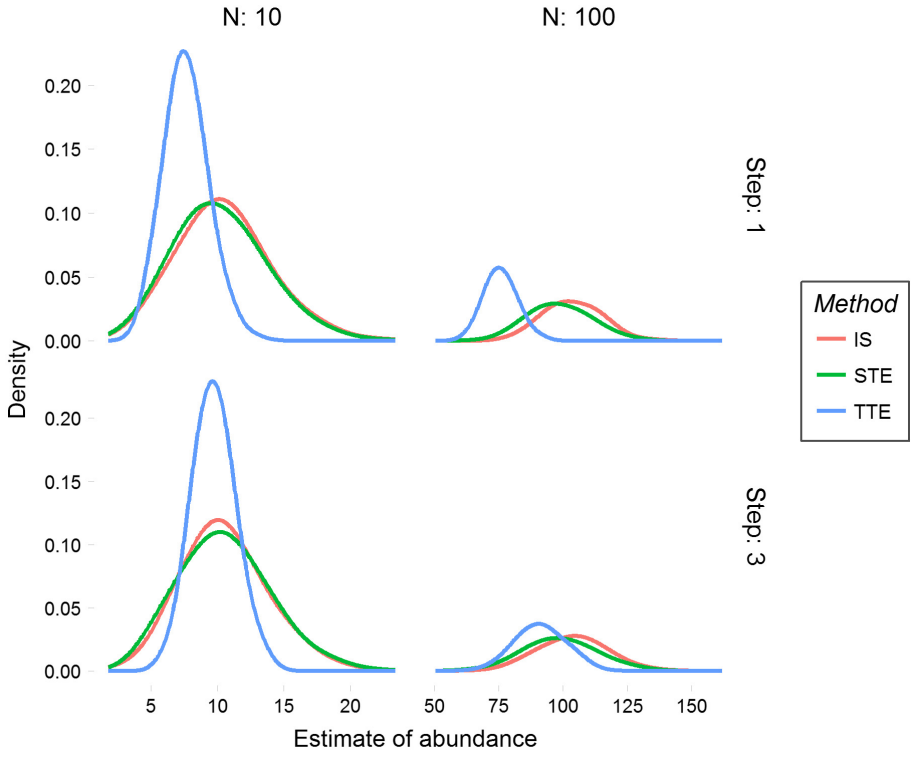

Fig. 4. Abundance estimates from simulated populations. We performed 1000 simulations for each of the three models at two step lengths for populations of size 10 (left column) and 100 (right column). Simulated animals took an uncorrelated random walk with step length 1 for the slow populations (top row) and step length 3 for the fast populations (bottom row).

Table 1. Abundance estimates and their standard errors from simulations for the three methods.

Method	N	Step	$\hat{N}$	Analytic SE($\hat{N}$)	SD($\hat{N}$)	Coverage (95% CI)
TTE	10	1	7.64	1.19	1.66	0.489
		3	9.71	1.35	1.6	0.881
	100	1	75.8	4.49	6.43	0.02
		3	91.2	5.06	9.66	0.524
STE	10	1	10.2	3.07	3.42	0.908
		3	10.6	3.13	3.39	0.913
	100	1	98.7	11.9	12.2	0.936
		3	99.1	11.9	14.2	0.899
IS	10	1	10.5	3.02	3.45	0.893
		3	10.6	3.05	3.21	0.931
	100	1	104	9.63	11.3	0.906
		3	104	9.65	13.3	0.843

Notes: IS, instantaneous sampling; STE, space to event; TTE, time to event; N: true abundance; Step: simulated step length; $\hat{N}$: mean estimated abundance; Analytic SE($\hat{N}$): analytic standard error using the delta method; SD($\hat{N}$): standard deviation of the abundance estimates from the 1000 simulations. We calculated 95% confidence intervals as $\hat{N} \pm 1.96 \cdot$Analytical SE ($\hat{N}$). Coverage is the proportion of 95% confidence intervals that overlapped true abundance.

the poor coverage of the 95% confidence intervals. In contrast, the analytic standard error and the standard deviation of the abundance estimates were similar for the STE and IS methods. The analytic standard error for these two methods was always slightly lower than the standard deviation of the abundance estimates. This is likely a feature of our particular dataset, but it may warrant further investigation whether the delta method systematically underestimates variance in these models. A Bayesian implementation of the STE model is straightforward and would eliminate the need for a delta method approximation. Interestingly, the variance and coverage were similar between the IS method and STE model for all combinations of step length and true abundance.

Case study

To evaluate the methods in a real-world setting, we applied them to camera data to estimate elk abundance. Because we applied these models to elk, which are viewed as a social animal, we first checked the assumption that animals move independently. The elk in our camera traps mainly appeared in groups of one or two, so we believe this assumption was reasonably well met (Fig. 5). For the TTE model,

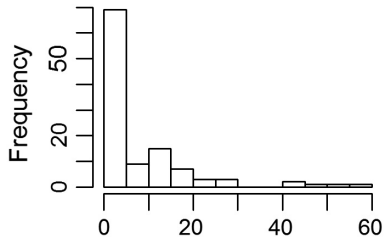

Fig. 5. Histogram of elk group size in the study area. We used photographs collected from February 1 to 13 and defined an elk group as the individuals in a burst of photographs separated from any other photographs of elk by at least 120 min. We counted every individual entering the frame as a new individual.

we recorded 101 elk detections over 80 cameras and 84 sampling occasions and estimated 2217 (standard error [SE] 211.6) elk (Fig. 6). For the STE model, we detected elk on 58 of the 288 sampling occasions and estimated abundance as 1718 (SE 225.6). Using the IS method, we observed elk in 60 of the 696 sampling occasions at the 80 cameras and we estimated 1613 elk. The standard error from the analytic estimator for the IS method was 530, and the standard error from the non-parametric bootstrap was 531. These abundance estimates were comparable to the 2009 aerial survey estimate of 2272 elk (IDFG, *unpublished data*). This aerial survey had no calculable standard error and only served as a rough estimate against which to compare our results.

Discussion

We derived the TTE model under a TTE framework to estimate abundance from the first animal detection at a given camera and sampling occasion. The model is functionally similar to the REM and has most of the same advantages and disadvantages. Most notably, both models require independent estimates of movement. The difference in confidence interval coverage between our fast and slow simulations demonstrated that the TTE model is sensitive to different movement speeds. This result prompted us to extend the TTE framework to develop the STE model. By collapsing the sampling occasions, the instantaneous nature of the STE makes it insensitive to movement. We further extended this idea

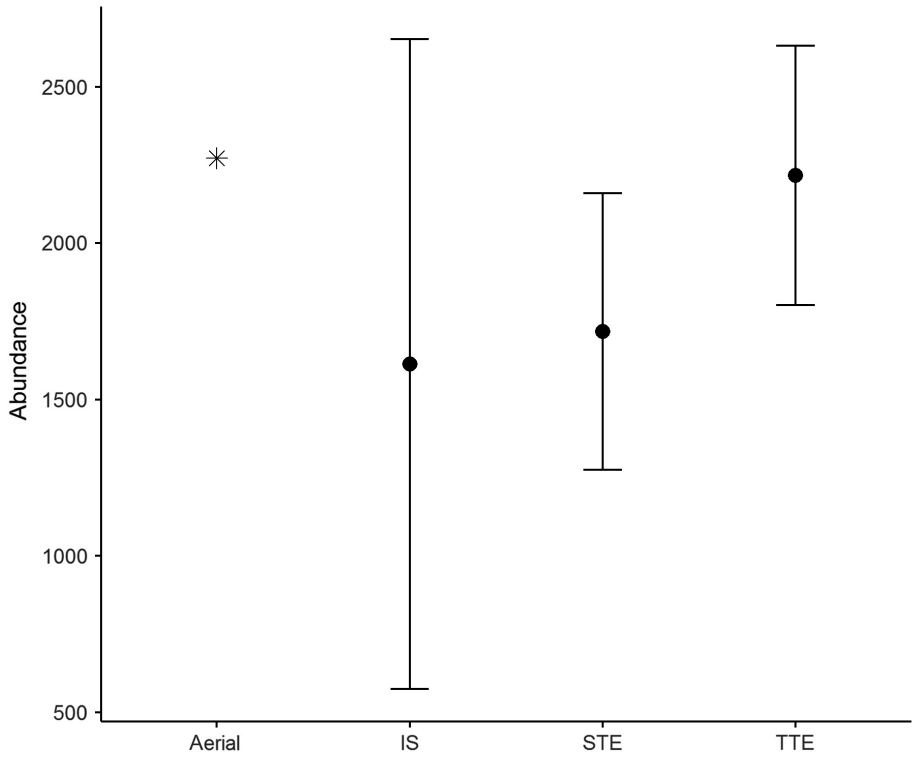

Fig. 6. Abundance estimates from all methods. Instantaneous sampling (IS), space to event (STE), and time-to-event (TTE) estimates of elk abundance are shown with their 95% confidence intervals, along with the 2009 aerial survey estimate (2272, standard error [SE] not calculable). The IS method estimated 1613 (SE 530), the STE model estimated 1718 elk (SE 225.6), and the TTE model estimated 2217 elk (SE 211.6).

to develop the IS estimator, which uses animal counts at each camera rather than the amount of area sampled. This is a novel application of fixed-area counts to cameras. By eliminating the Poisson assumption of the STE, this method gains flexibility but also requires accurate counts of animals in field settings. The assumptions and advantages of the three methods make them appropriate for different situations.

A major advantage of the IS and STE methods is the ability to eliminate variation in detection probability at cameras. They utilize time-lapse photographs, a form of camera data that have been largely overlooked. With motion-sensor cameras, a photograph of an animal at a certain time indicates that an animal was present. However, no photographs at that time mean either that no animals were present or that animals were present and not detected. Time-lapse photographs provide a complete log of animal presence and absence, so there is no need to model uncertainty in detection arising from equipment settings, environmental conditions, animal body size and distance, etc. Because the camera's detection zone is constant, we can easily define the area as the field of view. This is flexible enough to allow areas that vary across cameras within a study. Time-lapse photographs can be quite effective on relatively common species that are frequently detected, such as elk or deer.

The TTE model has the interesting advantage over any existing method in that it reduces the number of motion-sensor photographs required for analysis. The information at each camera and sampling occasion is contained in the time until the first animal detection, so the viewer can stop looking through pictures after the first detection. Currently, tens of thousands of remote cameras are deployed around the world, which produce millions of pictures (Steenweg 2017). Until photograph classification can be fully automated, large-scale camera trap studies are limited by the

hours required to classify millions of pictures. The TTE presents a unique way to decrease the workload and allowing quicker turnaround for abundance estimates.

One benefit of the STE and TTE models that should not be overlooked is that they allow us to estimate abundance without counting the number of animals in each photograph. Counts of animals in a photograph can provide some information about abundance, but they come with a cost of additional assumptions. Many species or conditions make it difficult to accurately count the number of animals, and group counts from photographs can be influenced by observer experience and photograph quality (Folsom 2017). For instance, behavior like rubbing against cameras can make it difficult to accurately count the number of animals in a given snapshot (Fig. 7). If we were to use counts in the STE model, we would see parallels between it, the IS estimator, and Poisson regression. However, since the STE was derived from hazard theory, we do not need to use these counts. Estimating abundance from the amount of space sampled before a species is detected is a novel application of TTE modeling.

There is great utility in the design-based inference underpinning the sampling for these models.

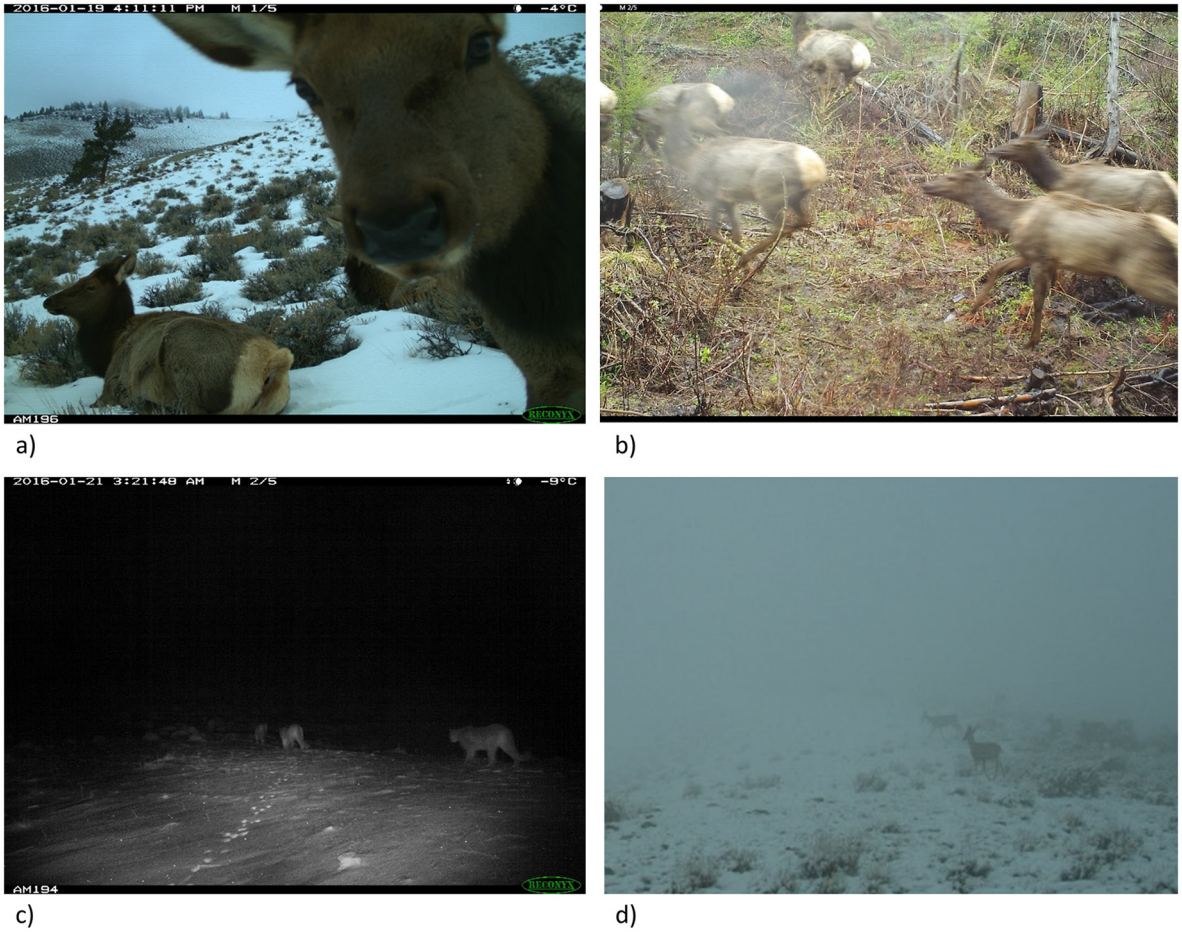

Fig. 7. Factors that influence accurate group counts. Various factors can influence accurate counts of group size, including animal behavior (a, b), photograph quality (c), and weather (d). Although it may be difficult to accurately count group size in these four photographs, the species is still identifiable. In studies where group counts are consistently difficult but species identification is possible, the space to event model is a useful tool to estimate abundance.

First, it allows us to easily extrapolate abundance from density. The area of interest is defined by the sampling frame, so there is no need to do post hoc estimates of sampling area, as have been criticized in many non-spatial capture–recapture studies (O'Brien 2011). Furthermore, the randomized design is useful for making inference to large areas. The models' power comes from the number of cameras deployed rather than the proportion of the landscape covered. Therefore, sampling can be performed at the scale of biological populations of large animals without requiring cameras in the home ranges of all animals. As with using time-lapse photographs, randomly placed cameras may be more useful for common species than for very rare or elusive animals. If it is difficult to collect enough data with randomly placed cameras, one may be able to apply a model-based design that applies prior knowledge of the species' movement or distribution instead.

The STE and TTE models assume that animals are distributed following a Poisson distribution at the camera level. For elk on a small spatial and temporal scale, this is a relatively realistic approximation of movement, but it may not apply to all species. It is worth noting that the REM and SC models make explicit assumptions about animal movement as well (Rowcliffe et al. 2008, Royle et al. 2014). Further simulations would be useful in determining how robust these methods are to violations of this assumption, especially by social or territorial species.

Our case studies used data from cameras that were deployed before these methods were fully developed. As such, the sampling design was not ideal, but we believe the estimates are reasonable. In future implementation, cameras should be deployed randomly rather than within a nested design. The nature of our camera array may have introduced autocorrelation between cameras in a cluster. However, we made efforts to distribute cameras within a plot so that no two were on the same road, trail, or ridge. We therefore believe the effect of autocorrelation was likely small. We recommend that future studies place cameras completely randomly, rather than by the combination of random, systematic, and subjective placement that we used. As noted earlier, we believe that elk movement was not greatly affected at the sub-cell scale because the sub-cells were quite homogeneous. However, studies in more heterogeneous areas should select sites randomly or systematically to avoid biasing estimates. Next, our cameras only took time-lapse photographs during daylight hours. We had to assume that if no motion-sensor photograph was taken, no elk were present. The most accurate way to decrease uncertainty in detection would be to take time-lapse photographs during the entire 24-h period. Many remote cameras can take both motion-triggered and time-lapse photographs, so this would not preclude collecting motion-triggered photographs for the TTE model or other uses. Finally, we were only interested in using prior aerial surveys as rough tests of the practicality and accuracy of these methods. We suggest a follow-up study that applies these methods in an area with a known abundance.

The TTE, STE, and IS methods represent a novel approach for estimating abundance of unmarked animals. They reframe the way we approach continuous, remotely collected data and mark a promising step toward completely noninvasive population monitoring. By using TTE modeling and time-lapse photographs, these models capture information that has largely been overlooked by previous camera trap methods. All three methods have broad applicability across many species with no natural identifying characteristics. Furthermore, they should be generalizable to any continuous-time remote trap whose detection area is calculable, such as acoustic detectors (Dawson and Efford 2009). While all the models have distinct advantages that make them appropriate for certain situations, we found that the STE model had the best precision in our field trial without the need for estimates of movement rate or group size counts.

Acknowledgments

Funding and support for this project were provided by the Idaho Department of Fish and Game, the Federal Aid in Wildlife Restoration Act, and the George and Mildred Cirica Graduate Student Support Fund at the University of Montana. We acknowledge the technicians and volunteers who made this work possible, along with the private landowners and federal land management agencies. Anna K. Moeller and Paul M. Lukacs conceived the ideas, and all authors designed the methodology and contributed to data collection. Anna K. Moeller performed the simulations, led the

analysis, and led the writing of the manuscript. All authors contributed critically to the manuscript and gave final approval for publication. The authors have no conflict of interests to declare.

Literature Cited

Balestrieri, A., A. Ruiz-González, M. Vergara, E. Capelli, P. Tirozzi, S. Alfino, G. Minuti, C. Prigioni, and N. Saino. 2016. Pine marten density in lowland riparian woods: a test of the Random Encounter Model based on genetic data. Mammalian Biology 81:439–446.

Barker, R. J., M. R. Schofield, W. A. Link, and J. R. Sauer. 2017. On the reliability of N-mixture models for count data. Biometrics 74:369–377.

Berkson, J. 1975. Do radioactive decay events follow a random Poisson-exponential? The International Journal of Applied Radiation and Isotopes 26:543–549.

Bischof, R., S. Hameed, H. Ali, M. Kabir, M. Younas, K. A. Shah, J. U. Din, and M. A. Nawaz. 2014. Using time-to-event analysis to complement hierarchical methods when assessing determinants of photographic detectability during camera trapping. Methods in Ecology and Evolution 5:44–53.

Bradshaw, C. J. A., D. W. Sims, and G. C. Hays. 2007. Measurement error causes scale-dependent threshold erosion of biological signals in animal movement data. Ecological Applications 17:628–638.

Burton, A. C., E. Neilson, D. Moreira, A. Ladle, R. Steenweg, J. T. Fisher, E. Bayne, and S. Boutin. 2015. Wildlife camera trapping: a review and recommendations for linking surveys to ecological processes. Journal of Applied Ecology 52:675–685.

Caravaggi, A., M. Zaccaroni, F. Riga, S. C. Schai-Braun, J. T. A. Dick, W. I. Montgomery, and N. Reid. 2016. An invasive-native mammalian species replacement process captured by camera trap survey random encounter models. Remote Sensing in Ecology and Conservation 2:45–58.

Carbone, C., et al. 2001. The use of photographic rates to estimate densities of tigers and other cryptic mammals. Animal Conservation 4:75–79.

Carbone, C., et al. 2002. The use of photographic rates to estimate densities of cryptic mammals: response to Jennelle et al. Animal Conservation 5:121–123.

Castro-Santos, T., and A. Haro. 2003. Quantifying migratory delay: a new application of survival analysis methods. Canadian Journal of Fisheries and Aquatic Sciences 60:986–996.

Chandler, R. B., and J. A. Royle. 2013. Spatially explicit models for inference about density in unmarked or partially marked populations. Annals of Applied Statistics 7:936–954.

Cox, D. R., and D. Oakes. 1984. Analysis of survival data. First edition. CRC Press, Boca Raton, Florida, USA.

Cusack, J. J., A. Swanson, T. Coulson, C. Packer, C. Carbone, A. J. Dickman, M. Kosmala, C. Lintott, and J. M. Rowcliffe. 2015. Applying a random encounter model to estimate lion density from camera traps in Serengeti National Park, Tanzania. The Journal of Wildlife Management 79:1014–1021.

Dawson, D. K., and M. G. Efford. 2009. Bird population density estimated from acoustic signals. Journal of Applied Ecology 46:1201–1209.

de Smith, M. J. 2015. STATSREF: statistical analysis handbook – a web-based statistics resource. The Winchelsea Press, Winchelsea, UK.

Dénes, F. V., L. F. Silveira, and S. R. Beissinger. 2015. Estimating abundance of unmarked animal populations: accounting for imperfect detection and other sources of zero inflation. Methods in Ecology and Evolution 6:543–556.

Efron, B., and R. J. Tibshirani. 1993. An introduction to the bootstrap. Chapman & Hall, New York, New York, USA.

Fewster, R. M., S. T. Buckland, K. P. Burnham, D. L. Borchers, P. E. Jupp, J. L. Laake, and L. Thomas. 2009. Estimating the encounter rate variance in distance sampling. Biometrics 65:225–236.

Folsom, C. 2017. Effect of photo quality on identification and count of populations in classifying camera trap photos. Senior Thesis. University of Montana, Missoula, Montana, USA.

Garrard, G. E., S. A. Bekessy, M. A. McCarthy, and B. A. Wintle. 2008. When have we looked hard enough? A novel method for setting minimum survey effort protocols for flora surveys. Austral Ecology 33:986–998.

Howe, E. J., S. T. Buckland, M.-L. Després-Einspenner, and H. S. Kühl. 2017. Distance sampling with camera traps. Methods in Ecology and Evolution 8:1558–1565.

Hutchinson, J. M. C., and P. M. Waser. 2007. Use, misuse and extensions of "ideal gas" models of animal encounter. Biological Reviews 82:335–359.

Jennelle, C. S., M. C. Runge, and D. I. MacKenzie. 2002. The use of photographic rates to estimate densities of tigers and other cryptic mammals: a comment on misleading conclusions. Animal Conservation 5:119–120.

Karanth, K. U. 1995. Estimating tiger *Panthera tigris* populations from camera-trap data using capture-recapture models. Biological Conservation 71:333–338.

Keever, A. C., C. P. McGowan, S. S. Ditchkoff, P. K. Acker, J. B. Grand, and C. H. Newbolt. 2017. Efficacy of N-mixture models for surveying and monitoring white-tailed deer populations. Mammal Research 62:413–422.

Kincaid, T. M., and A. R. Olsen. 2017. spsurvey: spatial survey design and analysis. R package version 3.4. https://CRAN.R-project.org/package=spsurvey

Manzo, E., P. Bartolommei, J. M. Rowcliffe, and R. Cozzolino. 2012. Estimation of population density of European pine marten in central Italy using camera trapping. Acta Theriologica 57:165–172.

Mood, A. M., F. A. Graybill, and D. C. Boes. 1974. Introduction to the theory of statistics. Third edition. McGraw-Hill, Singapore City, Singapore.

Muenchow, G. 1986. Ecological use of failure time analysis. Ecology 67:246–250.

O'Brien, T. G. 2011. Abundance, density and relative abundance: a conceptual framework. Pages 71–96 *in* A. F. O'Connell, J. D. Nichols, and K. U. Karanth, editors. Camera traps in animal ecology. Springer, Tokyo, Japan.

O'Connell, A. F., J. D. Nichols, and K. U. Karanth, editors. 2011. Camera traps in animal ecology: methods and analyses. Springer, Tokyo, Japan.

Oehlert, G. W. 1992. A note on the delta method. American Statistician 46:27–29.

Parsons, A. W., T. Forrester, W. J. McShea, M. C. Baker-Whatton, J. J. Millspaugh, and R. Kays. 2017. Do occupancy or detection rates from camera traps reflect deer density? Journal of Mammalogy 98:1547–1557.

Pyke, D. A., and J. N. Thompson. 1986. Statistical analysis of survival and removal rate experiments. Ecology 67:240–245.

R Core Team. 2015. R: a language and environment for statistical computing. R Foundation for Statistical Computing, Vienna, Austria.

Rovero, F., and A. R. Marshall. 2009. Camera trapping photographic rate as an index of density in forest ungulates. Journal of Applied Ecology 46:1011–1017.

Rowcliffe, J. M., C. Carbone, P. A. Jansen, R. Kays, and B. Kranstauber. 2011. Quantifying the sensitivity of camera traps: an adapted distance sampling approach. Methods in Ecology and Evolution 2:464–476.

Rowcliffe, J. M., J. Field, S. T. Turvey, and C. Carbone. 2008. Estimating animal density using camera traps without the need for individual recognition. Journal of Applied Ecology 45:1228–1236.

Rowcliffe, J. M., R. Kays, C. Carbone, and P. A. Jansen. 2013. Clarifying assumptions behind the estimation of animal density from camera trap rates. Journal of Wildlife Management 77:876.

Royle, J. A. 2004. N-mixture models for estimating population size from spatially replicated counts. Biometrics 60:108–115.

Royle, J. A., R. B. Chandler, R. Sollmann, and B. Gardner. 2014. Spatial capture–recapture. Elsevier, Waltham, Massachusetts, USA.

Samuel, M. D., E. O. Garton, M. W. Schlegel, and R. G. Carson. 1987. Visibility bias during aerial surveys of elk in northcentral Idaho. Journal of Wildlife Management 51:622–630.

Samuel, M. D., R. K. Steinhorst, E. O. Garton, and J. W. Unsworth. 1992. Estimation of wildlife populations ratios incorporating survey design and visibility bias. Journal of Wildlife Management 56:718–725.

Sasse, D. B. 2003. Job-related mortality of wildlife workers in the United States, 1937–2000. Wildlife Society Bulletin 31:1015–1020.

Sollmann, R., B. Gardner, R. B. Chandler, D. B. Shindle, D. P. Onorato, J. A. Royle, and A. F. O'Connell. 2013. Using multiple data sources provides density estimates for endangered Florida panther. Journal of Applied Ecology 50:961–968.

Steenweg, R., et al. 2017. Scaling up camera traps: monitoring the planet's biodiversity with networks of remote sensors. Frontiers in Ecology and the Environment 15:26–34.

Stevens, D. L., and A. R. Olsen. 2004. Spatially balanced sampling of natural resources. Journal of the American Statistical Association 99:262–278.

Thompson, S. K. 2002. Sampling. Second edition. John Wiley & Sons Inc, New York, New York, USA.

TrailcamPro. 2017. Reconyx game camera reviews. https://www.trailcampro.com

Whittington, J., M. Hebblewhite, N. J. Decesare, L. Neufeld, M. Bradley, J. Wilmshurst, and M. Musiani. 2011. Caribou encounters with wolves increase near roads and trails: a time-to-event approach. Journal of Applied Ecology 48:1535–1542.

Williams, B. K., J. D. Nichols, and M. J. Conroy. 2002. Analysis and management of animal populations. Academic Press, San Diego, California, USA and London, UK.

Zero, V. H., S. R. Sundaresan, T. G. O'Brien, and M. F. Kinnaird. 2013. Monitoring an endangered savannah ungulate, Grevy's zebra *Equus grevyi*: choosing a method for estimating population densities. Oryx 47:410–419.

Supporting Information

Additional Supporting Information may be found online at: http://onlinelibrary.wiley.com/doi/10.1002/ecs2.2331/full